Ocean Engineering 362 (2026) 126205

Contents lists available at ScienceDirect

Ocean Engineering

journal homepage: www.elsevier.com/locate/oceaneng

Research paper

Comparative study of ship fuel consumption prediction models based on multi-source operational and environmental data under dynamic ocean conditions

Cong Liu [a], Xiao Lang [b], Tsoulakos Nikolaos [c], Pentti Kujala [e], Mingyang Zhang [d,f,*]

[a] Department of Mechanical Engineering, Aalto University, Finland
[b] Department of Mechanical Engineering, Chalmers University of Technology, Sweden
[c] Laskaridis Shipping Co. Ltd., Athens, Greece
[d] MOE Key Laboratory of Marine Intelligent Equipment and System, Shanghai, China
[e] Estonian Maritime Academy, Tallinn University of Technology, Kopli 101, Tallinn, Estonia
[f] State Key Laboratory of Submarine Geoscience, Shanghai Jiao Tong University, Shanghai, China

ARTICLE INFO

Keywords:
Comparative study
Ship fuel consumption prediction
AI
Semi-empirical model
Physical model
Hydrometeorological conditions

ABSTRACT

Accurate prediction of ship fuel consumption is essential for improving maritime energy efficiency under variable hydrometeorological conditions. This study compares semi-empirical, physics-based, and artificial intelligence (AI)-based models using full-scale operational and environmental data from a Kamsarmax bulk carrier. The novelty of the work lies in the unified assessment of these three modelling methods under realistic and dynamic ocean conditions. The semi-empirical model estimates fuel use through resistance, propulsion efficiency, and engine fuel consumption relationships, while the physics-based model incorporates hydrodynamic, manoeuvring, and environmental effects. The AI model applies an attention-enhanced bidirectional long short-term memory network to learn nonlinear relationships from operational data. The comparative results show that the AI-based model provides the most accurate and stable predictions across unseen voyages, followed by the physics-guided model, whereas the semi-empirical model shows larger deviations under complex environmental conditions. These findings highlight the potential of AI-based prediction for fuel efficiency optimization and operational decision support, while physics-based modelling remains valuable for interpretation and diagnostic analysis.

1. Introduction

Maritime transport is a cornerstone of global trade, facilitating over 80% of worldwide cargo movement and playing a critical role in sustaining economic growth (UNCTAD, 2023). While the sector is often regarded as a relatively safe and energy-efficient mode of transportation (Kevin and Kodak, 2023; Probha and Hoque, 2018), it faces increasing pressure to decarbonize in line with the Paris Agreement's climate objectives (UNFCCC, 2022). According to the International Maritime Organization (IMO), shipping accounted for approximately 2.89% of global anthropogenic greenhouse gas (GHG) emissions in 2018 (IMO, 2020a; IMO, 2020b). Achieving the IMO's emission reduction targets requires both technological improvements in ship design and enhanced operational efficiency of existing vessels.

Accurate prediction of ship fuel consumption is fundamental to improving energy efficiency and reducing emissions in maritime transport. It supports a wide range of applications, including voyage optimization, performance monitoring, and decision-making for energy-efficient operations. A wide range of methods for estimating ship fuel consumption has been developed over the last few decades. These methods are typically categorized into three principal groups: empirical and semi-empirical approaches, physics-based models, and artificial intelligence (AI)-driven models.

Empirical and semi-empirical models are widely used due to their simplicity and computational efficiency. These approaches typically rely on regression-based formulations and simplified physical relationships to estimate ship fuel consumption. Key components include calm water resistance, viscous effects, and added resistance induced by environmental factors such as waves and wind (Lang and Mao, 2020; Molland et al., 2017). Classical methods such as the Holtrop and Mennen

This article is part of a special issue entitled: OE_Multi-Source Information Fusion published in Ocean Engineering.

* Corresponding author.
E-mail address: mingyang.zhang@sjtu.edu.cn (M. Zhang).

https://doi.org/10.1016/j.oceaneng.2026.126205
Received 14 April 2026; Received in revised form 9 May 2026; Accepted 21 May 2026
Available online 27 May 2026

(1982) model and ITTC-based approaches (ITTC, 2002), along with their subsequent developments incorporating operational data (Choi et al., 2010; Min and Kang, 2010; Manderbacka and Haranen, 2018), have been widely applied in practice. However, these models often rely on simplifying assumptions and may have limited capability in capturing complex nonlinear interactions under varying operational and environmental conditions.

Physics-based models provide a more detailed representation of ship hydrodynamics by explicitly modeling resistance components and propulsion mechanisms. These models consider the influence of environmental loads, such as waves and wind, and can achieve high accuracy under controlled conditions (Tillig and Ringsberg, 2019; Kim et al., 2023). Nevertheless, their application in real-world operations is often constrained by high computational costs and the need for detailed input parameters, which limits their scalability and real-time applicability.

With the increasing availability of onboard measurements and large-scale operational data, AI-based models have gained significant attention in recent years. Machine learning techniques, including regression models, neural networks, and deep learning methods, have demonstrated strong capabilities in capturing complex nonlinear relationships between ship fuel consumption and influencing factors such as speed, draft, environmental conditions, and operational states (Chen et al., 2023; Yan et al., 2020; Du et al., 2022a, 2022b). Recent studies have further advanced data-driven and hybrid modelling for ship performance prediction. Zhang et al. (2024) developed an attention-enhanced Bi-LSTM model for ship fuel consumption prediction using real operational data. Lang et al. (2024) proposed a physics-informed machine learning framework for ship speed prediction by combining physical constraints with data-driven learning. Grey-box and hybrid models have also been developed to improve prediction accuracy and extrapolation capability under complex operational conditions, including grey-box fuel consumption modelling (Fan et al., 2025), adaptive prediction frameworks for maritime energy management (Gao et al., 2025), dual-adaptive fuel consumption prediction (Lan et al., 2025), transfer-learning-based fuel consumption prediction (Luo et al., 2025), multi-algorithm feature selection for fuel consumption prediction (Piao et al., 2025). In addition, data-driven approaches have been increasingly applied to ship performance monitoring and degradation analysis, including the assessment of biofouling effects (Coraddu et al., 2019a, 2019b; Erol et al., 2020; Gupta et al., 2022; Lang et al., 2026). Despite their advantages, AI-based models may suffer from issues such as sensitivity to input data quality, lack of interpretability, and challenges in generalizing across varying operational conditions (Guo et al., 2026).

In practical applications, ship fuel consumption is influenced by complex and dynamic hydrometeorological conditions, including waves, wind, and ocean currents, as well as long-term performance degradation mechanisms such as biofouling (Schultz, 2007; Uzun et al., 2019; Valchev et al., 2022). These factors introduce significant variability and uncertainty in model predictions, making it challenging to evaluate model performance under realistic operating conditions. While individual modeling approaches have been extensively studied, there is still a lack of systematic comparative analysis of empirical, physical, and AI-based models using real operational data under changing metocean conditions.

To address this research gap, a comparative study of empirical, physics-based, and AI-driven methods for ship fuel consumption prediction is carried out under representative hydrometeorological conditions. The analysis is conducted using large-scale operational data from a bulk carrier operated by Laskaridis Shipping Co. Ltd. By evaluating the performance of different modeling approaches under realistic conditions, this study aims to provide a comprehensive understanding of their strengths, limitations, and applicability. The findings are expected to support the selection of appropriate modeling strategies for improving fuel efficiency and reducing emissions in maritime transport.

2. Full-scale case study ship

To evaluate the adopted typical semi-empirical, physical, and AI-based models, extensive operational data records from ship operational data from a Kamsarmax bulk carrier were employed, as detailed in Tables 1–5. The investigated vessel has a length overall of 229 m, a breadth of 32.26 m, and a deadweight of approximately 81,000 tons under summer load conditions, reflecting typical characteristics of large ocean-going bulk carriers. The hull form is characterized by a relatively high block coefficient (0.879), indicating a full-form vessel optimized for cargo capacity and fuel efficiency under loaded conditions, as shown in Table 1.

The propulsion system consists of a low-speed two-stroke diesel engine (HYUNDAI-MAN B&W 6S60ME-C8.5) with a maximum continuous rating (MCR) of 9930 kW, operating on heavy fuel oil (HFO). The engine performance characteristics, including specific fuel oil consumption (SFOC), provide a reliable basis for evaluating fuel consumption under different operational conditions, as shown in Table 2.

In addition, detailed hydrodynamic and geometric properties of the vessel, including wetted surface area, waterplane area, and stability-related parameters, are incorporated to support the development and validation of physical and semi-empirical models, as shown in Table 3. Key components of the propulsion system, such as the rudder and propeller, are also characterized by their geometric and performance parameters, including propeller diameter, blade number, wake fraction, and thrust deduction factor. These parameters are essential for accurately capturing resistance, propulsion efficiency, and maneuvering effects in physics-based and hybrid modeling approaches, see the details in Tables 4–5

The dataset is derived from real operational conditions, encompassing a wide range of loading states, speeds, and environmental conditions. Such comprehensive and high-resolution operational data provide a robust basis for systematically comparing the performance of empirical, physical, and AI-based models under realistic hydrometeorological conditions.

The dataset spans two years, from February 2021 to January 2023, and covers a broad range of operational and environmental conditions (Fig. 1). The corresponding dataset includes over one million samples collected under diverse operational and environmental conditions, with 266 parameters recorded for each sample (Zhang et al., 2024). The data were collected at 60-s intervals, providing high-resolution temporal information that is essential for capturing dynamic variations in ship performance. Such a comprehensive and high-frequency dataset enables a robust evaluation of the adopted semi-empirical, physical, and AI-based models under realistic operating conditions. The diversity of operational states and hydrometeorological conditions ensures that the models are assessed across a broad spectrum of scenarios, thereby enhancing the reliability, generalizability, and practical applicability of the comparative analysis.

Table 1
Ship specification of the Kamsarmax class bulk carrier.

Length overall	229.00 m
Length between perpendiculars	225.50 m
Breadth, moulded	32.26 m
Depth, moulded	20.05 m
Summer load line draught, moulded	14.45 m
Deadweight at summer load draught	80996.1 t
Draft (T)	12.6 m
Longitudinal Center of Gravity (XG)	−14.1 m
Block Coefficient (CB)	0.879
Vertical Center of Gravity (KG)	11.51 m
Metacentric Height (GM)	2.5 m

Table 2
Main characteristics of the main engine.

Manufacturer	HYUNDAI-MAN B&W
Type	6S60ME-C8.5
Maximum continuous rating (MCRME)	9930 kW × 90.4 rpm
Limited maximum continuous rating with engine power limitation (MCRME,lim)	8230 kW
SFOC at 75% of MCRME or 83% of MCRME lim	166.81 g/kWh
Number of engines	1
Fuel type	HFO

Table 3
Hydrodynamic properties.

Longitudinal Center of Flotation (LCF)	9.3 m
Longitudinal Metacentric Height (GML)	296.7247 m
Waterplane Area (AWP)	6981.6453 m^2
Wetted Surface Area (SWET)	12513.5261 m^2

Table 4
Main characteristics of the rudder.

Rudder Area in X (AX):	574.0 m^2
Rudder Area in Y (AY):	2050.0 m^2
Rudder Coordinates (XR, ZR):	−114.5, 10.5 m
Rudder Aspect Ratio (AR):	1.50
Rudder Angle (ARUD):	45.0 deg
Viscosity Coefficient (VISC):	1.27E-6 m^2/s
Rudder Gain (YRG):	0.0

Table 5
Main characteristics of the propeller.

Propeller Diameter (D)	6.95 m
Number of Propeller Blades (Z)	5.0
Added Mass Coefficient (KZZ)	0.0576
Added Mass Coefficient (KXX)	0.0033
Thrust Deduction Factor (TDF)	0.195
Wake Fraction	0.275
Developed area ratio (B)	0.52
Skew angle	24.5 deg
MCR	9930 KW

3. Methods

This section presents the methodologies adopted for predicting ship fuel consumption (SFC), encompassing three distinct approaches: semi-empirical models, physics-guided models, and deep learning models. Each method reflects a different level of abstraction and modeling philosophy, ranging from simplified empirical relationships to data-intensive learning frameworks, thereby forming a comprehensive evaluation framework, as illustrated in Fig. 2.

Semi-empirical methods combine theoretical principles with empirical data derived from both experimental studies and real ship operations. These models rely on established relationships between key variables such as ship speed, displacement, and resistance, enabling efficient and computationally inexpensive predictions. Due to their simplicity and interpretability, semi-empirical models are widely used in practical applications. Despite their practicality, their accuracy can become insufficient when the surrounding environmental conditions are complex and subject to substantial variation.

Physical models focus on representing the ship's hydrodynamic behavior under varying sea conditions through detailed mathematical formulations. By incorporating resistance components, propulsion characteristics, and environmental forces such as waves and wind, these models provide a more rigorous and physically consistent description of ship performance. While capable of achieving high accuracy, physical models often require significant computational resources and detailed input data, which may limit their applicability in large-scale or real-time scenarios.

Deep learning models utilize artificial intelligence techniques to predict SFC by learning complex patterns and nonlinear relationships directly from large datasets. These models are particularly effective in handling high-dimensional data and capturing interactions among multiple influencing factors, including operational conditions and hydrometeorological variables. However, their performance is highly dependent on data quality and quantity, and they may lack physical interpretability compared to traditional approaches.

By integrating these three modeling paradigms within a unified framework, this study enables a systematic comparison of their predictive capabilities, robustness, and applicability under real hydrometeorological conditions. The comparative analysis aims to identify the strengths and limitations of each approach, providing guidance for selecting appropriate models in practical maritime applications.

3.1. Semi-empirical model

The propulsion system of a ship primarily encompasses energy consumption for propulsion, auxiliary systems, and heating. Fig. 3 illustrates the workflow for the fuel consumption estimation by semi-empirical methods. Ship fuel consumption under real sea conditions is governed by a combination of factors, including engine operating characteristics, propeller properties, and the resistance imposed on the ship. The propulsion power demand is related not only to ship speed but also to the prevailing operating conditions. Conventionally, the estimation process for propulsion power and fuel consumption is performed sequentially, beginning with the evaluation of ship resistance and followed by the calculation of the required power. Resistance at different sailing speeds may be estimated using model tests, numerical techniques, or semi-empirical methods. Moreover, the added resistance arising from wind and wave effects, which is frequently encountered during normal operation, should be considered in the total resistance. The total resistance should be balanced by the thrust generated by the

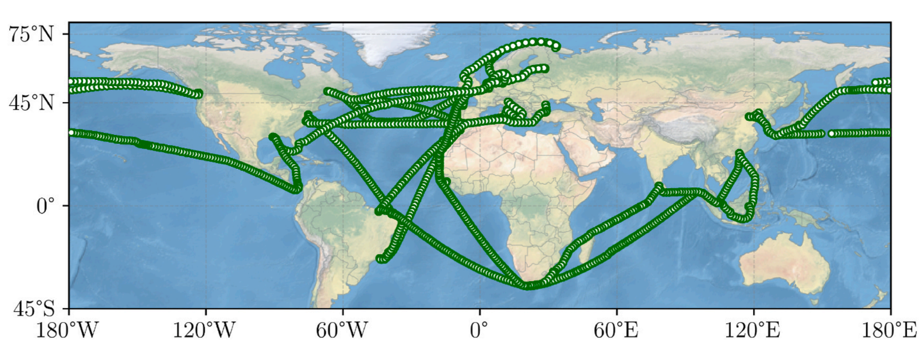

Fig. 1. Ship trajectories of the bulk carrier from January 2021 to February 2023.

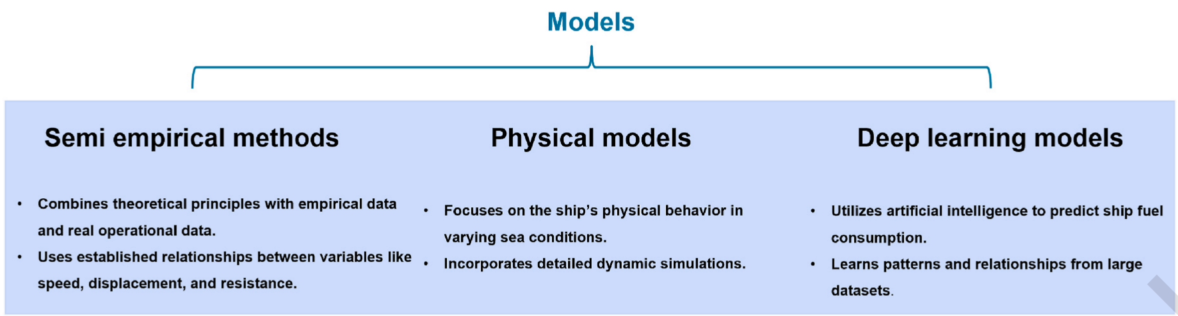

Fig. 2. Ship fuel consumption prediction models used in the comparative study.

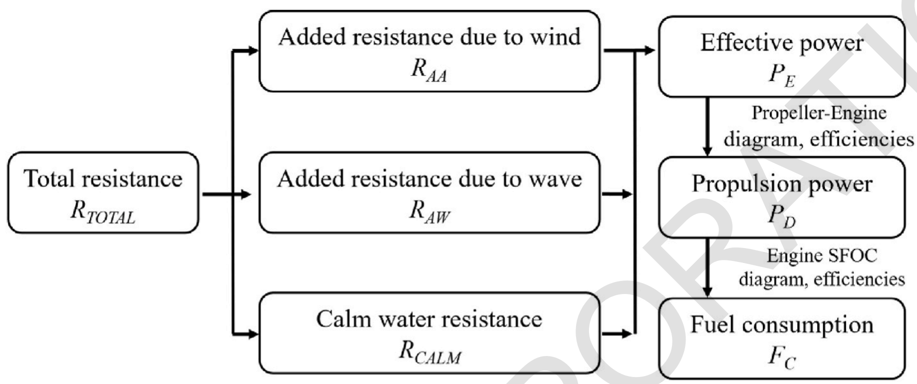

Fig. 3. Workflow for fuel consumption estimation using the semi-empirical model.

propulsion system and engine.

The total resistance of a ship in actual navigation is represented as the sum of calm water resistance, added resistance due to wind, and waves. Holtrop and Mennen (1982) proposed an approximate method for estimating calm water resistance based on ship geometry and characteristics. The calm water resistance (R_{CALM}) is the sum of several components as

$$R_{CALM} = R_F(1+k_1) + R_{APP} + R_W + R_{other}, \tag{1}$$

where frictional resistance R_F is evaluated according to the ITTC-1957 standard method (ITTC, 2002). The remaining resistance contributions, namely appendage resistance (R_{APP}), wave resistance (R_W), and other terms are estimated on the basis of empirical relations or available test results. In this work, R_{APP}, R_W, and R_{other} were derived from the experimental data of the case study ship described in Section 2.

The added resistance due to wind R_{AA} is influenced by both the exposed area of the ship's superstructure and the relative wind. According to the ISO (2015), the R_{AA} can be determined as follows

$$R_{AA} = \frac{1}{2}\rho_A\left[C_{AA}(\varphi_{WR})A_{XV}{V_{WR}}^2 - C_{AA}(0)A_{XV}{V_g}^2\right], \tag{2}$$

where ρ_A is the air density, and A_{XV} is the transverse projected area of the vessel above the waterline. In addition, V_{WR} and V_g denote the relative wind speed and ship speed over ground. The parameter C_{AA} represents the wind resistance coefficient modified as a function of the relative wind direction (φ_{WR}).

The added resistance due to waves (R_{AW}) is evaluated through the combination of wave spectrum and transfer functions. For irregular waves, the corresponding expression is given by

$$R_{AW}(\omega|H_s,T_p,\gamma,V,\beta) = 2\int_0^{\infty}\int_{-\frac{\pi}{2}}^{+\frac{\pi}{2}} S(\omega|H_s,T_p,\gamma)\frac{R_{aw}(\omega|V,\beta)}{\zeta_a(\omega)^2}D(\theta-\beta)d\theta d\omega, \tag{3}$$

where S denotes the wave spectrum, which is described by the significant wave height (H_s) and the peak period (T_p). The parameter β represents the relative wave direction, whereas $D(\theta)$ refers to the directional spreading function defined as follows

$$S(\omega|H_s,T_p,\gamma)D(\theta) = \frac{320{H_s}^2}{T_p^4\omega^5}exp\left(\frac{-1950}{{T_p}^4\omega^4}\right)\gamma^{exp\left[\frac{-(\omega-\omega_p)^2}{2\sigma^2\omega_p^2}\right]}D(\theta), \tag{4}$$

$$D(\theta) = \begin{cases} \frac{2}{\pi}\cos^2(\theta) & \text{for } -\frac{\pi}{2} \le \theta \le \frac{\pi}{2} \\ 0 & \text{otherwise} \end{cases} \tag{5}$$

In this study, the wave added resistance transfer function R_{aw} is calculated using the ITTC (2014) semi-empirical method. On the basis of the total resistance determined from Eqs. (2)–(5), the effective power (P_E) required to balance the overall resistance (R_{TOTAL}) at a specified speed (V) is given in Eq. (6). Subsequently, Eqs. (6) and (7) present the formulation for brake power (P_B) calculation as

$$P_E = R_{TOTAL}\cdot V, \tag{6}$$

$$P_B = \frac{P_D}{\eta_s} = \frac{P_E}{\eta_s\cdot\eta_h\cdot\eta_r\cdot\eta_o}, \tag{7}$$

where P_D denotes the propulsion power, while η_s, η_h, η_r, and η_o represent the efficiencies associated with the shaft, ship hull, relative rotation, and open water characteristics. By combining the SFOC with the corresponding operating time, the fuel consumption under different working conditions can be calculated.

Finally, Eq. (8) is used to determine the ship fuel consumption as

$$SFC = \frac{3600 \times P_B \cdot SFOC}{1000 \times \rho}. \tag{8}$$

Here, SFC is expressed in L/h, while ρ represents the fuel density. The term SFOC is commonly given in g/kWh, indicating the fuel mass required to produce one kW-h of engine power. In the paper, the initial SFOC is shown in Table 2, and the real value is updated by real ship fuel consumption records.

Overall, to estimate fuel consumption using above empirical formulas, a total of 22 parameters are required as mentioned in Eqs (1)–(8). These include components for resistance calculations, such as calm water resistance R_{CALM}, wind resistance R_{AA}, and wave-induced resistance R_{AW}, which together require 16 parameters of the target ship (e.g., air density, projected area, wave spectrum characteristics, and relative speeds). Additionally, propulsion power estimation involves 4 efficiency-related parameters ($\eta_s \cdot \eta_h \cdot \eta_r \cdot \eta_o$), while fuel consumption calculation requires 2 parameters: the SFOC and operational duration. These parameters are crucial to accurately determine ship fuel usage under real sea conditions.

3.2. Physics-guided ship fuel consumption prediction models

The developed ship physical method for evaluating ship performance integrates comprehensive environmental and operational data with advanced ship manoeuvring systems modelling and machine learning techniques to provide accurate and reliable forecasts. The framework outlined in the diagram systematically addresses various aspects of ship operation, combining them into a cohesive process that enhances prediction accuracy and operational efficiency, see Fig. 4.

The following explanation delineates each component of the framework, highlighting their roles and interactions.

1) Input data collection

The framework begins with the collection of extensive input data during the voyage. This data is categorized into three main segments: (a) Environmental Conditions: Parameters such as sea depth, wave height, wave period, wave direction, wind speed, wind direction, current direction, and current speed are crucial. These variables provide a detailed understanding of the external forces acting on the ship. (b) Waypoint Definition: The latitude and longitude coordinates that define the ship route. This geospatial data is essential for mapping the ship route and integrating environmental conditions specific to each location. (c) Operational Conditions: Information on the ship speed and mean draft. These operational parameters are vital for assessing ship performance and fuel consumption under different conditions.

2) 6-DoF time domain physics-based model

The core of the framework is the Six Degrees of Freedom (6-DoF) time domain physics-based model. This model can be used to simulate the main characteristics of the target ship and her manoeuvring systems. This model simulates ship motions under varying sea conditions by considering the environmental and operational inputs. It outputs several critical performance metrics: (a) Fuel consumption, (b) 6 DOF ship motions, (c) Environmental forces acting on the ship, (d) Propeller RPM, (e) Propeller thrust, and (f) Delivered power. These outputs provide a detailed assessment of the ship's performance, helping in understanding how different factors or ship motions influence fuel consumption.

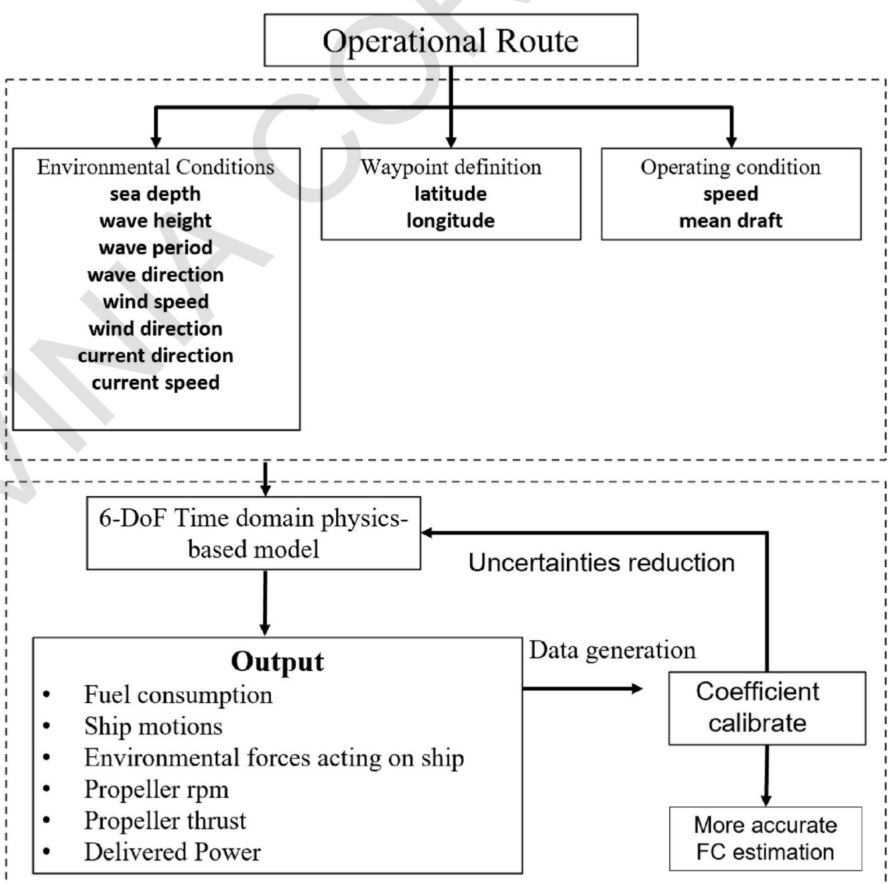

Fig. 4. Framework for developing the physics-based model for ship performance evaluation.

3) Uncertainty reduction and coefficient calibration

To calibrate the coefficients of the ship physical model, the framework incorporates uncertainty reduction techniques and machine learning (ML) training. The uncertainty reduction techniques of the 6-DoF model are used to calibrate coefficients using the regression method based on the historical operational records of the case study ship. This process involves: (1) Refining the parameters of a 6-DoF model to minimize errors and improve the reliability of predictions compared to the actual operations of the target ship. (2) Leveraging regression method to learn patterns and relationships between inputs and outputs. This step is crucial for improving the predictive accuracy of the fuel consumption prediction model. The integration of physics-based modeling and ML techniques leads to more accurate fuel consumption estimations. The calibrated coefficients and trained models are used to refine the initial predictions of the specific ship, providing more precise and reliable outputs. This iterative process ensures that the model remains robust and adaptive to varying conditions.

The ship physical method framework combines detailed environmental and operational data with sophisticated modeling and machine learning approaches to predict ship fuel consumption accurately. By systematically addressing the complexities of ship operations and environmental interactions, this method provides valuable insights for optimizing fuel usage, reducing operational costs, and promoting sustainable maritime practices. This comprehensive approach underscores the importance of integrating multiple data sources and advanced analytical techniques in maritime research and ship operation optimization.

3.2.1. The 6-DoF ship dynamics model

3.2.1.1. Overview of the modelling framework. In this study, the semi-empirical model is formulated as a quasi-steady one-degree-of-freedom (1-DOF) longitudinal force-balance approach. It estimates the total resistance acting along the ship's sailing direction, and then converts the required effective power into fuel consumption using propulsion efficiency and SFOC correction. Therefore, this model does not explicitly solve the coupled ship motion equations, or manoeuvring-induced dynamic effects. Accurate prediction of ship fuel consumption under realistic operational conditions requires a consistent integration of vessel dynamics, hydrodynamic forces, propulsion characteristics, and environmental loads. To this end, a physics-guided modelling framework is adopted, in which a six degrees-of-freedom (6-DoF) manoeuvring model serves as the core dynamic engine.

The 6-DoF model simultaneously resolves the coupled translational and rotational motions of the vessel, namely surge, sway, heave, roll, pitch, and yaw, while incorporating the effects of propulsion, steering, and environmental disturbances. Compared with reduced-order manoeuvring models (e.g.,3-DoF), the present formulation enables a more comprehensive representation of energy dissipation mechanisms, which are directly linked to fuel consumption.

The overall modelling workflow integrates ship-specific parameters (hull, propeller, rudder), operational inputs (speed, heading, control commands), and environmental conditions (wind, waves, current, resulting in time-resolved predictions of vessel motion and propulsion demand. The nature of the physics model for ship fuel consumption predictions is a 6-DoF ship manoeuvring model. The workflow of this 6-DoF ship manoeuvring model is illustrated in Fig. 5.

3.2.1.2. Governing equations of 6-DoF motion. The ship dynamics are formulated in the body-fixed coordinate system using Newton-Euler equations. The general form of the 6-DoF equations can be expressed as Eq. (10)

$$M(\nu)\dot{\nu} + C(\nu)\nu + D(\nu)\nu + g(\eta) = \boldsymbol{\tau}, \tag{10}$$

where $\nu = [u, v, w, p, q, r]^T$ denotes the velocity vector, $\eta = [x, y, z, \phi, \theta, \psi]^T$ represents the position and orientation, $\boldsymbol{M}$ is the mass and added mass matrix, $\boldsymbol{C}$ accounts for Coriolis and centripetal effects, $\boldsymbol{D}$ represents nonlinear hydrodynamic damping, $\boldsymbol{g}$ denotes hydrostatic restoring forces, and $\boldsymbol{\tau}$ is the generalized external force vector.

In the present model, the detailed expansion of these equations follows the formulation in Taimuri et al. (2020), where inertia coupling, nonlinear damping, and hydrostatic restoring effects are explicitly included. A key feature of the model is the strong coupling tween degrees of freedom. For instance, sway and yaw motions are inherently coupled through hydrodynamic derivatives, while roll motion is manoeuvring performance and energy dissipation.

3.2.1.3. Hydrodynamic force decomposition. The total external force vector T is decomposed into several physically interpretable components, as Eq. (11) shows

$$\tau = \tau_{hull} + \tau_{\mathrm{prop}} + \tau_{\mathrm{rudder}} + \tau_{\mathrm{wind}} + \tau_{\mathrm{wave}} + \tau_{\mathrm{current}}. \tag{11}$$

(1) Hull hydrodynamic forces

Hull forces are modeled using nonlinear manoeuvring derivatives, including linear, quadratic, and cubic terms of sway velocity and yaw rate. As shown in Taimuri et al. (2020), these forces take the general form as Eq. (12)

$$X_{Hull}, Y_{Hull}, N_{Hull} \sim v, r, v^2, r^2, vr, v^3, r^3. \tag{12}$$

This formulation reflects the inherently nonlinear nature of viscous

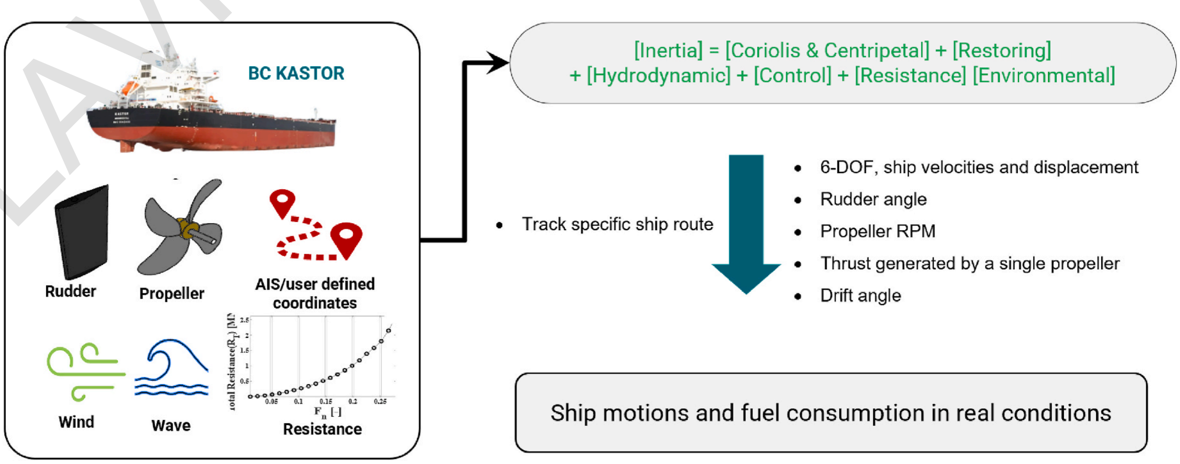

Fig. 5. Flowchart of the 6-DOF ship dynamics model for ship fuel consumption prediction.

flow around the hull. Importantly, manoeuvring-induced velocities introduce additional resistance, which contributes significantly to fuel consumption.

(2) Propeller thrust and hull-propeller interaction

The propeller thrust is modeled as Eq. (13)

$$X_{prop} = \rho n^2 D^4 K_T, \tag{13}$$

where the thrust coefficient K_T depends on the advance ratio. The effective inflow velocity is corrected using the wake fraction as Eq. (14)

$$V_A = (1-w)U. \tag{14}$$

Furthermore, thrust deduction is considered to account for hull-propeller interaction. These corrections reflect the fact that propulsion efficiency is not constant but depends on the flow field around the stern.

(3) Rudder forces and propeller slipstream effects

Rudder forces are calculated based on local inflow velocities, which include contributions from both ship motion and propeller slipstream. The axial and lateral velocities at the rudder are given by $V_{X,R}, V_{Y,R}$. The resulting lift and drag forces depend on the effective angle of attack, which is influenced by flow straightening effects. This highlights the strong coupling between propulsion and steering systems.

(4) Environmental loads

Wind loads are computed using semi-empirical aerodynamic formulations (e.g., Blendermann method), accounting for relative wind speed and direction. Short-wave-induced forces are modeled using second-order mean drift formulations, integrated along the ship waterline. These forces are proportional to wave amplitude squared and depend on encounter angle. Shallow water modifies resistance, added mass, and hydrodynamic derivatives. As shown in the Taimuri et al. (2020), correction factors are introduced to account for depth-to-draft ratio effects.

3.2.1.4. Energy-based interpretation for fuel consumption. A key advantage of the 6-DoF framework is that it enables a physically consistent linkage between vessel dynamics and fuel consumption. The propulsion power is given by as Eq. (15)

$$P = T \cdot U, \tag{15}$$

where the required thrust T balances total resistance as Eq. (16)

$$T = R_{calm} + R_{maneuver} + R_{wave} + R_{wind} + R_{shallow}. \tag{16}$$

Among these components, manoeuvring-induced resistance is particularly important and can be expressed as a function of sway velocity and yaw rate as Eq. (17)

$$R_{maneuver} \sim v^2 + r^2 + vr. \tag{17}$$

This implies that steering actions, course corrections, and environmental disturbances directly increase energy dissipation. Consequently, fuel consumption is not solely a function of forward speed but also of dynamic motion states.

To ensure computational efficiency, several simplifying assumptions are adopted in the present model. Hydrodynamic forces are represented using quasi-steady formulations, while heave, roll, and pitch motions are assumed to be small and therefore linearized. In addition, memory effects associated with radiation forces are neglected, and short waves are considered to primarily influence in-plane motions. These assumptions are consistent with established formulations and make the model suitable for real-time simulation and large-scale operational analysis. However, it should be noted that they may limit prediction accuracy under extreme sea states or highly unsteady conditions. Within this framework, the model can be interpreted as a physics-informed reduced-order model. Although the governing equations are derived from first principles, key parameters, such as hydrodynamic derivatives and interaction coefficients, are calibrated using experimental measurements and operational data. This hybrid modeling strategy ensures physical consistency while improving generalization capability and enabling adaptability across different vessel types and operating conditions.

Overall, the developed 6-DoF ship dynamics model provides a unified and physically grounded framework for simulating vessel motion and estimating fuel consumption under realistic environmental and operational scenarios. By explicitly resolving the coupled interactions among ship dynamics, hydrodynamic forces, and environmental loads, the model captures the fundamental energy dissipation mechanisms governing fuel usage. As such, this physics-guided approach offers a robust foundation for further integration with machine learning techniques, enabling enhanced prediction accuracy and facilitating advanced operational optimization.

The 6-DoF ship dynamics model is designed to predict fuel consumption and assess vessel performance by incorporating environmental factors, waypoint definitions, and operational parameters. This physics-based framework evaluates the impact of external conditions and dynamic ship responses. Wind-related inputs include speed and angle relative to an earth-fixed reference frame, while shortwave data encompass wave height, period, and direction. In extreme scenarios, aerodynamic forces significantly influence ship behavior, with wind loads calculated using the Blendermann method (Blendermann, 1994). The model also integrates shallow water effects and shortwave forces, as described by Taimuri et al. (2020). Comprehensive ship-specific details for the dynamics model are provided in Section 2.

Based on these inputs, the vessel trajectory is governed by an autopilot control system (Zhang et al., 2023). The rudder adjusts the course to maintain the desired heading set via AIS data. A Proportional Derivative (PD) controller determines the target rudder angle (δ_T) to align the ship heading (ψ_d) as defined by Eq. (18) (Matusiak, 2021). The autopilot controller uses a linear differential equation (Eq. (19)) to calculate rudder adjustments, where ω_δ represents the rudder's turning rate. To achieve the target speed (U_d), a P-controller modulates the ship propeller revolutions. Initially, the propeller rotational speed is set based on the vessel current speed (U), as outlined in prior research (ITTC, 2002). The updated propeller rotation rate ($N_{rps_{new}}$) is calculated using Eq. (20), derived from navigation data and desired operational conditions as

$$\delta_T = K_p(\psi - \psi_d) + K_D\dot{\psi}, \tag{18}$$

$$\dot{\delta} = sgn(\delta - \delta_T)\omega_\delta, \tag{19}$$

$$N_{rps_{new}} = \frac{-k_{T1}V_A\rho D^3 + \sqrt{\left(k_{T1}V_A\rho D^3\right)^2 + 4k_{T0}\rho D^4\left(V_A^2\rho D^2 k_{T2} - X_{Prop_{new}}\right)}}{2k_{T0}\rho D^4}, \tag{20}$$

where K_P and K_D denotes the gain coefficients. While k_{T0}, k_{T1}, and k_{T2} are 2nd-order polynomial coefficients used to describe the propeller thrust characteristic for a propeller of diameter of D. $X_{Prop_{new}}$ is the desired propeller thrust at the ship advanced speed of V_A ($V_A = (1-w)U_d$).

Based on these quantities, the updated propeller rotational speed (RPS) N_{rps_i} is defined as Eq. (21)

$$N_{rps_i} = K_{p_{rev}}(U_d - U) + N_{rps_{new}}, \tag{21}$$

where $K_{p_{rev}}$ refers to the proportional gain used in the P-controller. As a result, the model is able to reproduce ship control inputs, including rudder angle and propeller RPM, together with vessel motion behavior influenced by environmental conditions in realistic operating scenarios.

3.2.2. Ship fuel consumption calculations

This comprehensive data collection enables detailed analysis and understanding of the ship performance under various operational conditions, facilitating optimized ship handling and fuel efficiency, see more in the previous paper (Zhang et al., 2024) and the data in Fig. 1 and Section 2. Based on the 6-DoF ship dynamics model, utilizing the specified input data, the model can generate the following outputs: 6-DOF ship velocities and displacement, Rudder angle, Propeller RPM, thrust generated by a single propeller, Drift angle of the vessel. Then, the total power required of the target ship can be calculated by using Eq. (22). Finally, ship fuel consumption is obtained from Eq. (8). In this model, the initial value is set to 1 g/kWh and will be updated based on the specifications of the target ship as

$$Power = Thrust \times Z \times V, \tag{22}$$

where Z represents the number of propellers and V denotes the vessel's surge speed.

The physical model for ship fuel consumption prediction of the selected case study ship encompasses a comprehensive set of parameters spanning multiple domains, including ship geometry, stability, propulsion, rudder characteristics, environmental conditions, and operational settings. Specifically, ship geometry and stability parameters involve key dimensions such as length, breadth, draft, and coefficients like block coefficient and metacentric heights. The propulsion system parameters cover engine performance metrics, propeller characteristics, and efficiency coefficients. Rudder parameters include rudder area, aspect ratio, and control gains, while environmental conditions account for wind, wave, and current characteristics. Operational parameters incorporate ship speed, simulation time, and thrust coefficients. Overall, the model integrates approximately 76 parameters, reflecting its comprehensive nature and the level of detail required for accurate predictions of ship performance and fuel cost under actual operating conditions.

3.3. Deep learning model

This section develops a deep learning approach for predicting ship fuel consumption in real-world operation based on Bidirectional Long Short-Term Memory (Bi-LSTM) networks with attention mechanisms, as illustrated in Fig. 6. The model leverages the strengths of Bi-LSTM, which effectively captures both past and future dependencies, and attention mechanisms, which enhance the model's ability to focus on the most relevant portions of the data streams. This combination enables the model to efficiently capture and utilize historical information, delivering robust predictive performance. The procedure of the algorithm is described from data preparation to final prediction in Fig. 6 and Table 6. Fig. 7 shows that the proposed fuel consumption prediction model contains four core modules, namely an input layer, Bi-LSTM layers, attention layers, and an output layer. More comprehensive details are reported in Zhang et al. (2024).

Although the original high-frequency dataset contained 266 measured parameters, the final AI-based surrogate model did not use all variables as direct inputs. Following the Decision Tree-based feature-importance analysis, the Bi-LSTM model with an attention mechanism used 14 input variables, including ship speed over ground, ship course, ship heading, ship mean draft, trim, main engine shaft power, main engine temperature, significant wave height, wind speed, current speed, wind direction, wave direction, current direction, and air temperature (Zhang et al., 2024). The output variable was ship fuel consumption.

The model was developed using historical high-frequency operational data collected from February 2021 to January 2023. During model development, the historical dataset was internally divided into training and validation sets. In addition, 5-fold cross-validation was adopted for hyperparameter tuning and validation. The trained model was subsequently tested using operational data streams collected from February 2023 to June 2023. Therefore, the final testing was based on chronologically separated, voyage-based data rather than a random split. This strategy ensures that the test set was not mixed with the training or validation data, thereby avoiding potential data leakage in the ship operational data.

This study introduces a deep learning model, designed for high-precision prediction tasks. The model consists of four main parts: an

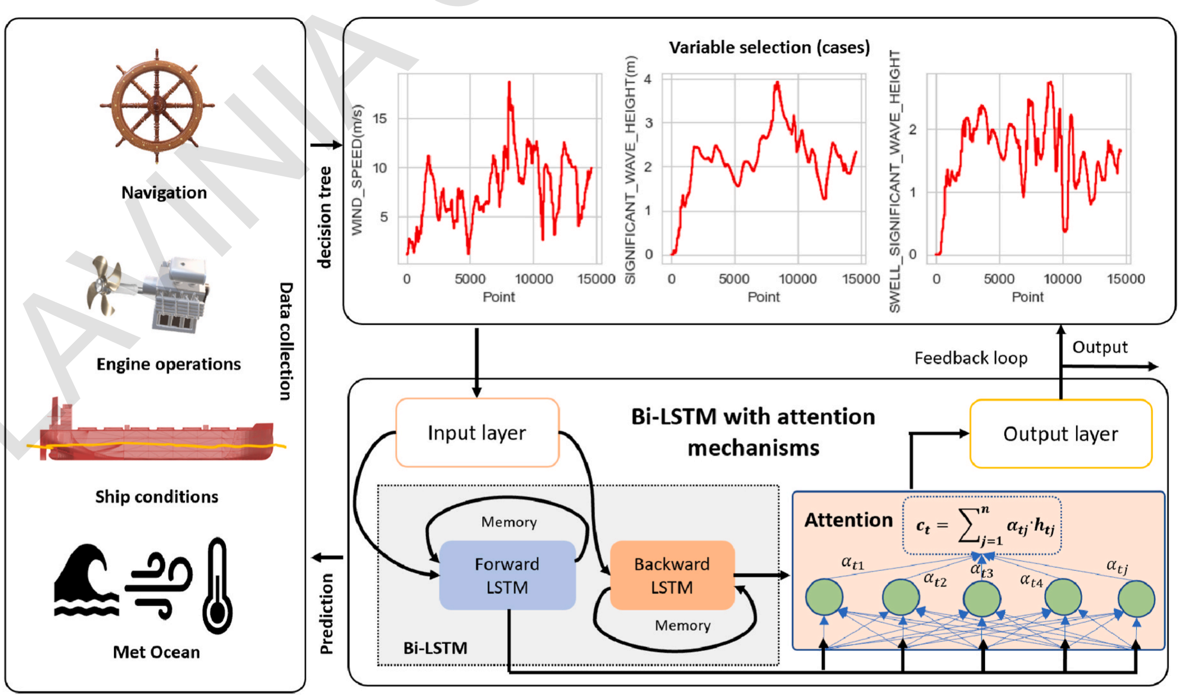

Fig. 6. Architecture of the deep learning method for ship fuel consumption prediction.

Table 6
Procedure of the Bi-LSTM model with an attention mechanism for ship fuel consumption estimation.

Algorithm: Bi-LSTM with attention mechanisms for ship fuel consumption (SFC) prediction
1 **Input:** Data collection SFC(n), see more in Section 2.1
2 **Output:** AI-based ship fuel consumption surrogate model
3 Select key variables X(n) and ship fuel consumption SFC (n) in the time domain
4 Split the training data set $data_{train}$ and $data_{test}$ from X(n) using k folds cross-validation method.
5 For batch $data_{batchsize}$ in $data_{train}$
6 For L-length data $data_l$ in $data_{batch\ size}$
7 For $i = 1$ to L
8 Using forward LSTM to an encoder $\overrightarrow{h_t}$
9 Using backward LSTM to an encoder $\overleftarrow{h_t}$
10 End For
11 Compute Attention score α_{tj} and c_t
12 Compute ship fuel consumption SFC_t from c_t
13 End For
14 Training the model to identify ship energy system in real operational conditions
15 End For
16 Save the prediction model: AI-based ship fuel consumption prediction model

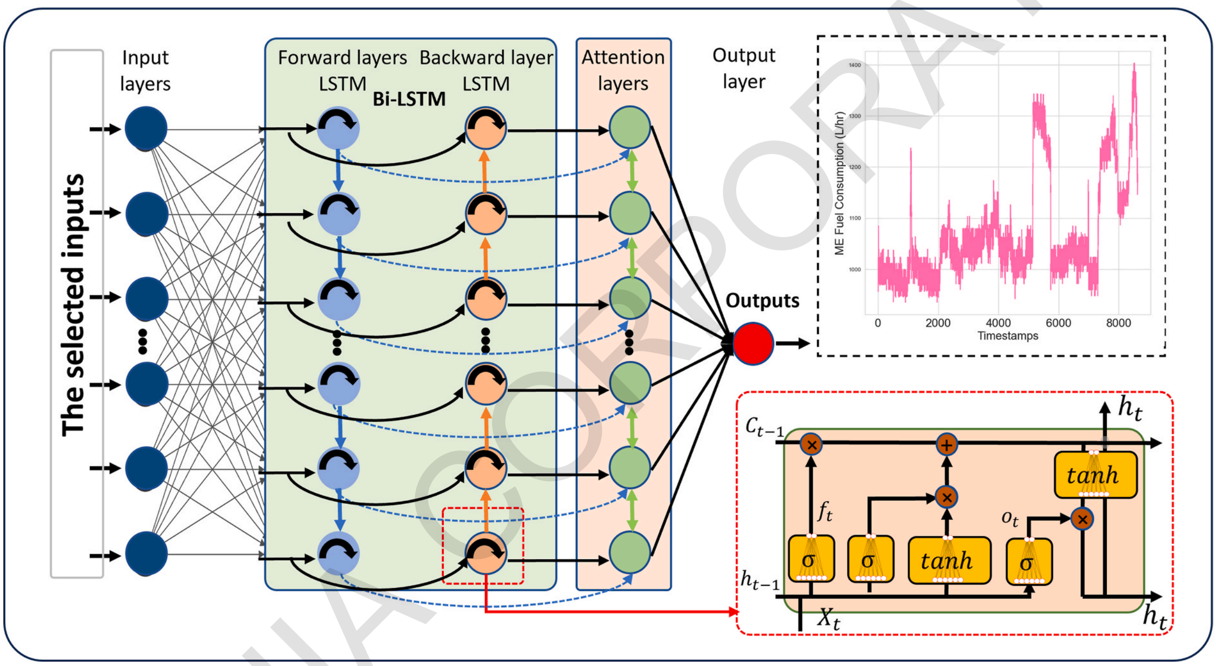

Fig. 7. Network architecture of the attention-enhanced Bi-LSTM model for ship fuel consumption prediction.

input layer, three stacked Bi-LSTM layers, three attention layers, and an output layer. For each Bi-LSTM layer, 128 hidden units were assigned. In addition, the attention mechanism was employed to strengthen the model's capability to focus on informative features. Hyperparameter tuning was carried out using grid search in combination with 5-fold cross-validation. The final configuration includes the Adam optimizer, a learning rate of 5e-5, a batch size of 48, a dropout rate of 0.2, a regularization parameter of 0.1, and training over 178 epochs with early stopping (patience = 10). The total number of trainable parameters is 722,433 in this model.

4. Results and discussion

4.1. Data for comparative study

To validate the predictive accuracy of the three models introduced in Section 3, namely, the semi-empirical, physical, and AI-based models, data from a single laden voyage (Voyage 1) was employed, as shown in Fig. 10. Voyage 1 was part of the chronologically separated external test dataset collected after the AI model-development period, and was therefore treated as unseen voyage. This voyage spanned the route from Vancouver, Canada, to Yantai, China, covering a total distance of 7223.90 nautical miles. Over the course of this voyage, a dataset consisting of 28,479 records was collected, capturing a broad spectrum of operational and environmental conditions. The data was recorded at regular intervals, ensuring high-resolution temporal granularity essential for robust model validation. Each record includes parameters critical to ship fuel consumption prediction, such as ship speed, draft, propulsion system metrics, and environmental conditions (e.g., wave height, wind speed, and current velocity). These parameters provide a comprehensive dataset for evaluating the models under realistic operational scenarios. However, certain challenges were encountered during the data preprocessing phase. Due to missing values in some parts of the dataset, only the first 19,000 data points, which were deemed complete and reliable, were used for model validation. Missing values were handled through estimation methods based on interpolation and statistical imputation to ensure data integrity. This subset was selected to minimize the impact of incomplete data on the model evaluation, ensuring a fair and consistent comparison across the three approaches.

The use of this dataset allowed for an in-depth assessment of the model performance under real-world conditions, providing a strong foundation for evaluating their predictive accuracy and robustness. The error metrics computed for each model, based on this voyage data, are presented in the subsequent sections to highlight the relative strengths and weaknesses of each approach.

4.2. Ship fuel consumption using semi-empirical model

The semi-empirical model demonstrated moderate accuracy in predicting ship fuel consumption, with a mean prediction error of −17.32%, an MSE of 75,589.01, and an RMSE of 274.93, as shown in Fig. 8. This model, based on simplified equations derived from historical data and theoretical principles, effectively balances computational efficiency and practical application. However, its performance is hindered by an inability to capture complex, nonlinear interactions inherent in real-world operational conditions. The model's underestimation of fuel consumption highlights its limitations in representing dynamic environmental factors, such as fluctuating wave and wind conditions. As a result, while the semi-empirical model is suitable for quick estimations or scenarios with limited data availability, its applicability to high-precision tasks is limited.

4.3. Ship fuel consumption using physical model

The physical model achieved significantly improved results compared to the semi-empirical approach, with a mean prediction error of 7.02%, an MSE of 23,754.37, and an RMSE of 154.12, as shown in Fig. 9. By incorporating detailed hydrodynamic principles and environmental data, the model effectively captures critical factors such as wave-induced resistance, aerodynamic forces, and ship maneuvering dynamics. This higher level of physical fidelity allows for more accurate predictions under diverse and challenging operational conditions. Such capabilities make the physical model an excellent choice for detailed performance evaluations and scenario analyses in maritime operations. However, the noticeable underestimation around waypoints 16000–17500 can be mainly explained by the relatively severe wave conditions encountered during that voyage segment. Under such conditions, the increase in added resistance becomes highly nonlinear, and the coupled effects of waves and vessel motion are difficult to fully capture using the present physics-based model. In addition, uncertainty in environmental input data may further contribute to the observed deviation. At other waypoints, the physics-based model generally tends to overestimate fuel consumption. This systematic positive bias may be attributed to the simplifications and assumptions made in the physical modelling framework. In particular, the use of calibrated or empirical values for propulsion efficiency, wake fraction, thrust deduction, and hydrodynamic coefficients may not fully reflect voyage-specific variations in draft, trim, speed, and sea state. As a result, the effective propulsion efficiency may be underestimated, or the resistance contribution may be overestimated, leading to higher predicted fuel consumption.

Beyond predicting fuel consumption, the physical model demonstrates its versatility by simulating ship trajectories and 6-DOF motions. For example, as shown in Fig. 10, the orange trajectory represents the actual voyage path of Voyage 1, while the blue trajectory reflects the predicted path using the physical model. The close alignment between the two trajectories underscores the model's ability to simulate ship behavior under real hydrometeorological conditions, accounting for environmental interactions and operational constraints. The distinct peak in surge velocity observed around the middle of the voyage can be associated with a manoeuvring or route-adjustment segment identified from the ship trajectory. During this period, transient changes in engine, propeller thrust, and rudder action, have caused a short-term increase in surge velocity.

However, the physical model's reliance on high-quality input data and precise calibration introduces challenges, particularly in real-time applications. The computational demands for processing complex simulations can also limit its practicality in scenarios requiring rapid decision-making. Despite these limitations, the physical model remains a robust and reliable tool for maritime engineering, offering not only accurate fuel consumption predictions but also the ability to simulate detailed ship dynamics and operational scenarios. This dual capability positions the physical model as an indispensable resource for both predictive and diagnostic analyses in maritime operations.

4.4. Ship fuel consumption using AI based surrogate model

The prediction results shown in Fig. 11 were obtained from the eight complete unseen voyages arranged in chronological order, and these data were not used for model training, or cross-validation. The AI-based surrogate model outperformed both the semi-empirical and physical models, achieving a mean prediction error of just −0.51%%, an MSE of 2834.49, and an RMSE of 53.24, as shown in Fig. 11. Utilizing a Bi-LSTM network with attention mechanisms, this model excelled in capturing complex, nonlinear relationships between operational and environmental parameters. Its ability to process large datasets and adapt to diverse conditions highlights its transformative potential for maritime

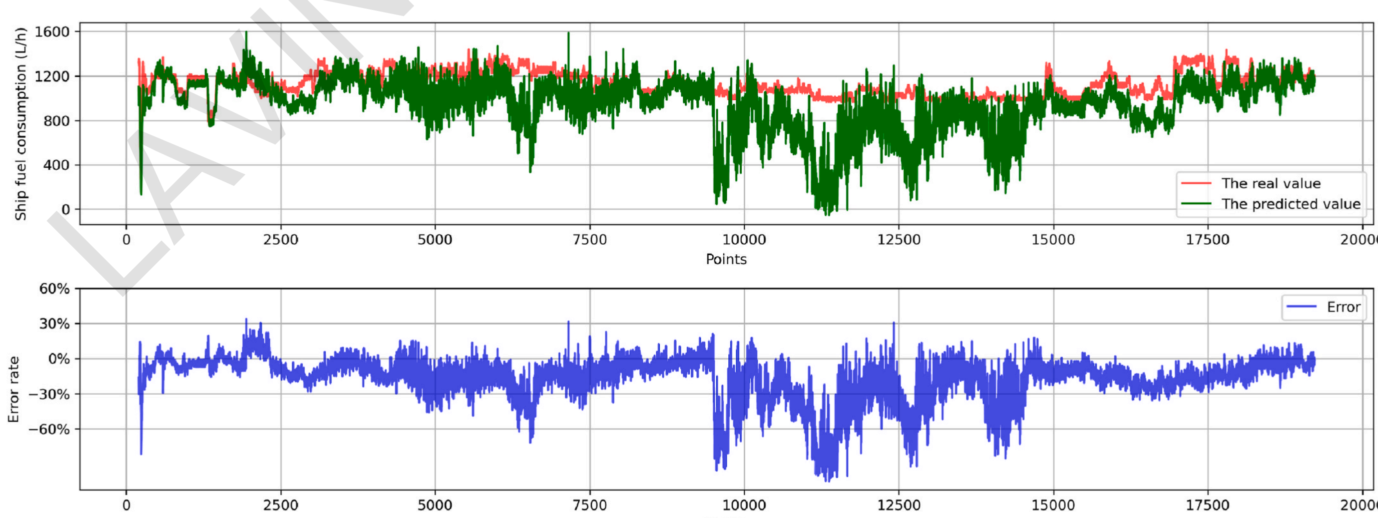

Fig. 8. Error analysis of ship fuel consumption prediction using the semi-empirical model.

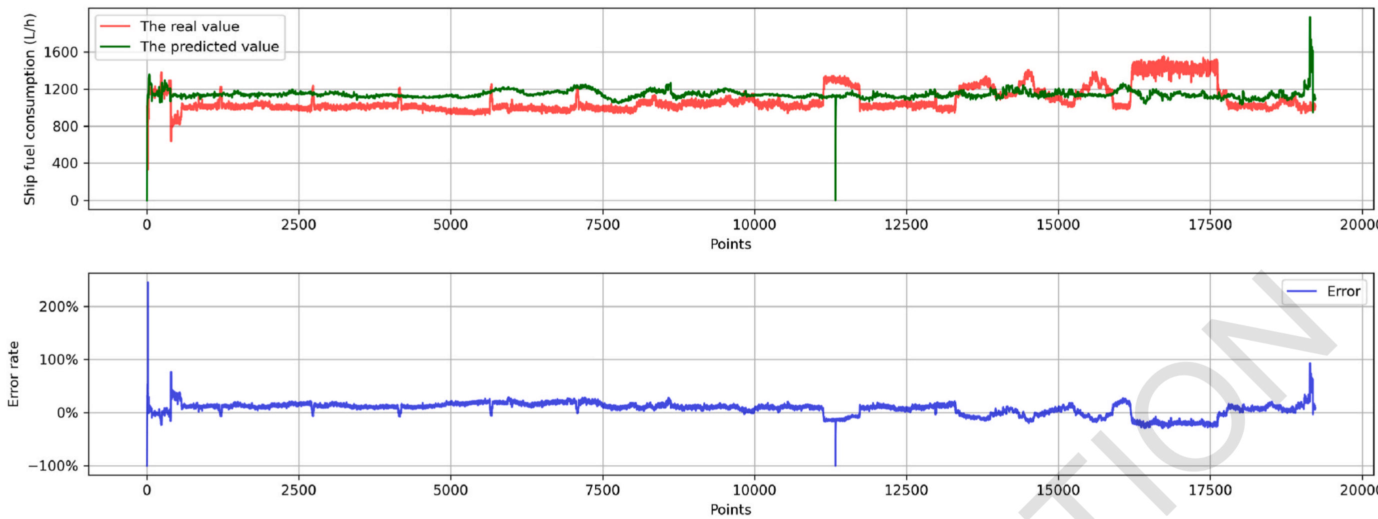

Fig. 9. Error analysis of ship fuel consumption prediction using the physics-based model.

applications. The AI model scalability and accuracy make it ideal for real-time optimization and decision-making. However, its reliance on high-quality, extensive datasets and its "black-box" nature pose challenges in interpretability and transparency. While the AI-based approach is poised to redefine predictive modeling in maritime engineering, its application must be carefully managed to address these limitations.

4.5. Comparative studies for different voyages

To further evaluate the robustness and generalization capability of the three models introduced in Section 3, namely the semi-empirical, physical, and AI-based surrogate models, a comprehensive comparative study was conducted using data from eight full-scale voyages under varying operational conditions. These voyages, summarized in Fig. 12, include both laden and ballast conditions and cover diverse geographical routes and environmental scenarios, thereby providing a representative dataset for cross-validation. The selected voyages span a wide range of sailing distances, from short regional routes (e.g., Voyage 2: 980.22 nm) to long intercontinental voyages (e.g., Voyage 1: 7223.90 nm), with the number of recorded data points ranging from 6081 to over 28,000. This diversity ensures that the models are tested across different ship loading conditions, hydrometeorological environments, and operational profiles, including variations in wave conditions, wind fields, and ocean currents.

Using the developed semi-empirical, physical, and AI-based surrogate models, fuel consumption predictions were generated for all eight voyages. Fig. 13 illustrates the associated fuel consumption trends of the mentioned ship voyages for unseen data.

The comparative results across multiple voyages reveal fundamental differences in the modeling mechanisms of the three approaches. The semi-empirical model consistently has the largest prediction error, indicating that simplified formulations fail to capture the cumulative effects of environmental disturbances and maneuvering-induced resistance. In particular, the neglect of nonlinear interactions between ship motion and external loads leads to systematic deviation, especially under complex sea states and dynamic operating conditions.

The physical model improves prediction accuracy by explicitly incorporating hydrodynamic processes, reducing RMSE by approximately 40% compared to the semi-empirical approach. However, the presence of a relatively large RMSE suggests that uncertainties in hydrodynamic coefficients, environmental inputs, and model calibration propagate through the simulation. This highlights an inherent limitation of physics-based models. While they provide interpretable and physically consistent predictions, their accuracy strongly depends on the quality of input data and parameter estimation. In addition, the computational cost associated with solving coupled nonlinear dynamics limits their applicability for real-time or large-scale deployment.

In contrast, the AI-based surrogate model achieves the lowest RMSE (55.08 L/h), demonstrating its ability to capture complex nonlinear relationships that are difficult to represent explicitly in traditional models. The significant reduction in RMSE, approximately 78% compared to the semi-empirical model and 63% compared to the physical model, indicates that data-driven approaches can effectively learn hidden patterns in operational and environmental interactions. Furthermore, the consistent performance across unseen voyages suggests strong generalization capability, which is critical for practical deployment in real-world maritime applications.

From a methodological perspective, these findings highlight that no single modeling approach is universally optimal. Instead, the results suggest that hybrid frameworks combining physics-based constraints with data-driven learning offer a promising direction for future research. Such approaches could leverage the interpretability of physical models while retaining the predictive power of AI, thereby improving robustness, accuracy, and applicability in ship fuel consumption prediction.

5. Conclusions

This study presents a comprehensive comparative analysis of semi-empirical, physics-based, and AI-based surrogate models for predicting ship fuel consumption under realistic hydrometeorological conditions, using extensive operational data from a Kamsarmax bulk carrier across multiple global voyages. The results reveal clear differences in predictive performance, which can be attributed to both the number of parameters considered and each model's capability to represent nonlinear interactions between ship dynamics and environmental forcing.

The semi-empirical model, utilizing only 22 parameters, demonstrates high computational efficiency but limited predictive capability, yielding an average RMSE of 247.71 L/h. The relatively low number of parameters constrains the model's ability to capture complex system behaviors, particularly nonlinear coupling effects between environmental loads and ship motion, leading to systematic underestimation under realistic sea conditions.

The physics-based model incorporates a substantially higher level of detail, with 76 parameters, enabling improved representation of hydrodynamic processes, maneuvering dynamics, and environmental interactions. This results in a reduced average RMSE of 147.32 L/h. The increased number of parameters enhances the model's physical fidelity

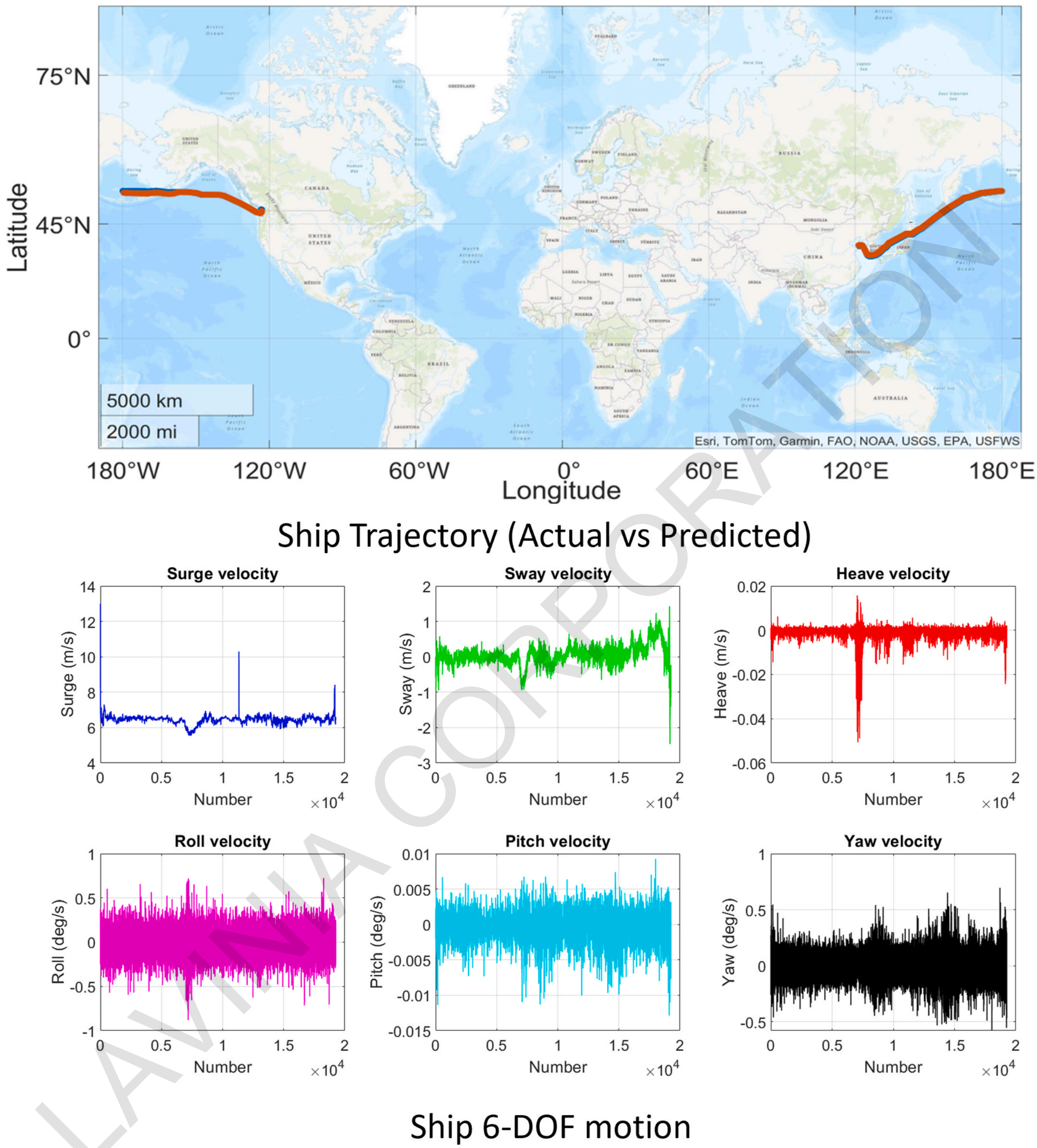

Fig. 10. Actual and predicted ship trajectories and ship motions obtained using the physics-based model.

and adaptability across different operating conditions, including transitions between laden and ballast states. However, this also introduces sensitivity to input data quality and parameter calibration, as well as increased computational cost.

The AI-based surrogate model leverages large-scale datasets, effectively learning from over one million implicit features extracted from high-resolution operational data. This high-dimensional representation allows the model to capture complex nonlinear relationships without explicitly defining physical mechanisms, resulting in the best performance among all approaches, with an average RMSE of 55.08 L/h. Compared to the semi-empirical and physics-based models, it reduces RMSE by approximately 78% and 63%, respectively. This demonstrates that increasing model complexity, when supported by sufficient data, can significantly enhance predictive capability.

Overall, the results indicate that model performance is strongly influenced by the balance between parameterization and physical

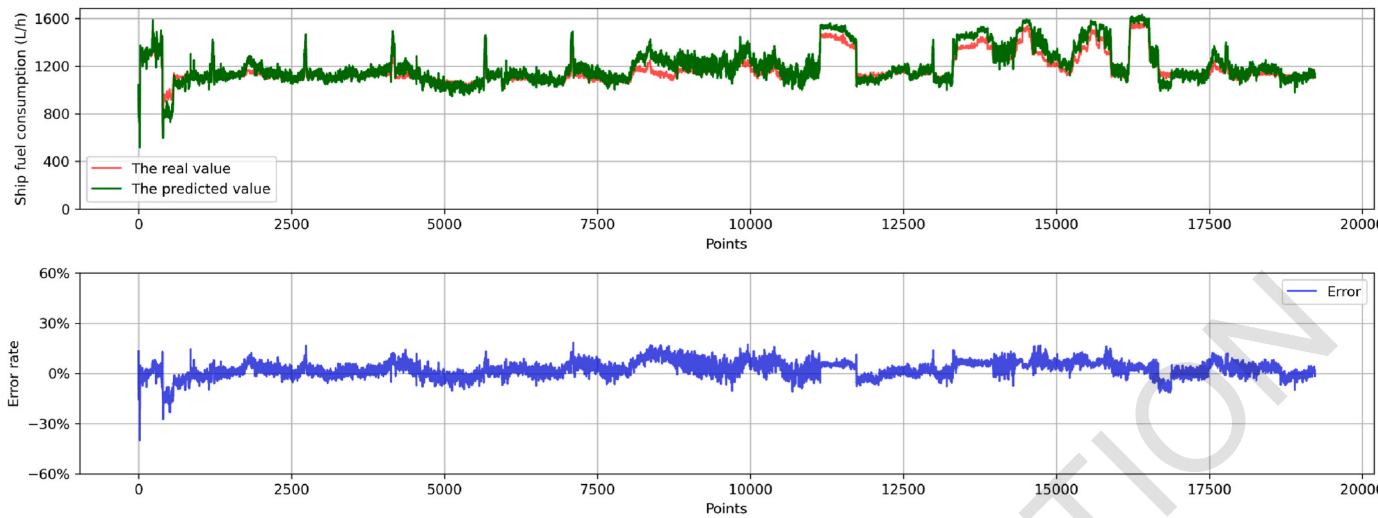

Fig. 11. Error analysis of ship fuel consumption prediction using the deep learning model.

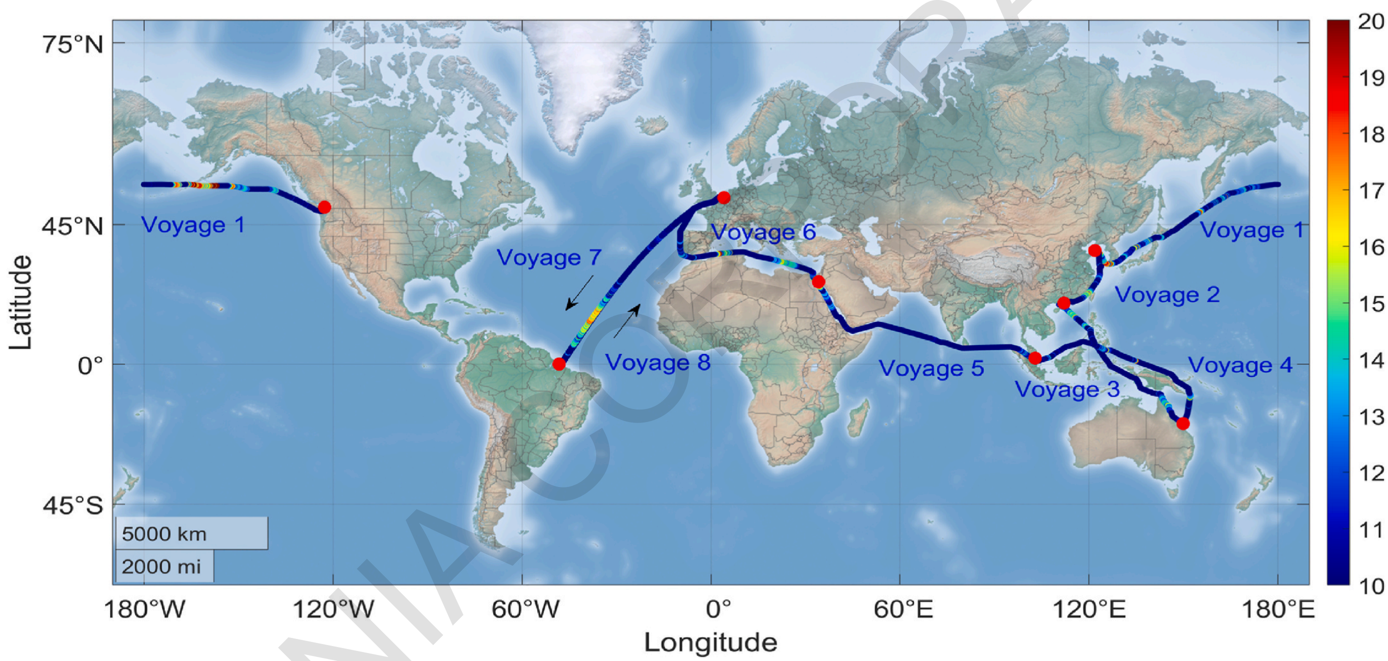

Fig. 12. Distribution of voyages used for the comparative study.

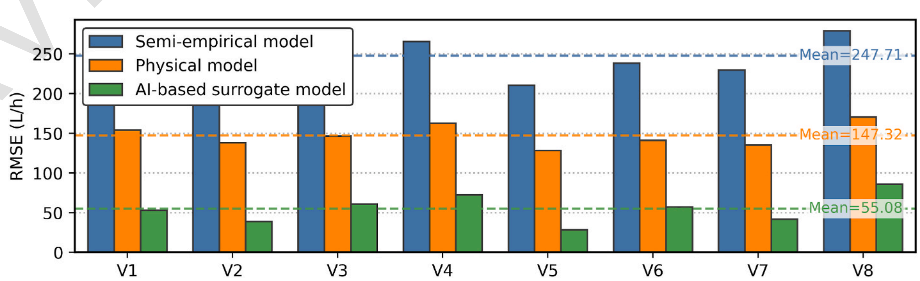

Fig. 13. Comparison of RMSE for the semi-empirical, physical, and AI-based surrogate models across eight unseen voyages.

interpretability. While models with fewer parameters offer computational efficiency, they lack sufficient expressiveness to capture complex system dynamics. Conversely, models with higher parameterization improve accuracy but introduce challenges related to calibration, data dependency, and computational cost. The AI-based model represents an extreme case of high-dimensional parameterization, achieving superior accuracy at the expense of interpretability. However, several limitations of the present comparative study should be acknowledged. First, the AI-based surrogate model depends strongly on the quality and volume of the training data. Sensor noise, missing values, abnormal fuel flow measurements, and underrepresented operating or environmental conditions may reduce its reliability when the model is applied to unseen scenarios. The Bi-LSTM model also remains less interpretable than semi-empirical and physics-guided formulations, which limits its diagnostic capability. Third, all three modeling approaches are affected by uncertainties in environmental inputs, including wave, wind, and current information. Such uncertainties may propagate into resistance estimation, vessel dynamic response, and fuel consumption prediction.

These findings suggest that future research should focus on hybrid modeling frameworks that combine physics-based structures with data-driven learning. Such approaches can leverage a moderate number of physically meaningful parameters while incorporating data-driven corrections to improve accuracy, thereby achieving an optimal balance between interpretability, robustness, and predictive performance. A key limitation of this study is the lack of direct validation of the 6-DoF motion predictions due to the absence of full-scale motion measurements. Future work should incorporate real-world motion sensing data and explore physics-informed AI approaches to enhance model transparency and reliability. These developments are expected to support scalable and intelligent solutions for maritime fuel efficiency optimization.

CRediT authorship contribution statement

Cong Liu: Writing – review & editing, Writing – original draft, Visualization, Validation, Software, Methodology, Investigation, Formal analysis, Conceptualization. **Xiao Lang:** Writing – review & editing, Methodology, Investigation, Formal analysis, Conceptualization. **Tsoulakos Nikolaos:** Writing – review & editing, Formal analysis, Data curation, Conceptualization. **Pentti Kujala:** Writing – review & editing, Supervision, Investigation, Formal analysis. **Mingyang Zhang:** Writing – review & editing, Writing – original draft, Investigation, Funding acquisition, Formal analysis, Conceptualization.

Declaration of competing interest

The authors declare that they have no known competing financial interests or personal relationships that could have appeared to influence the work reported in this paper.

Acknowledgements

This work was supported by the National Natural Science Foundation of China (NSFC) under Grant No. 52501441, and National Natural Science Fund for Excellent Young Scientists Fund Program (Overseas) under Grant No. 24FAA02373. The views expressed in this paper are solely those of the authors and do not necessarily reflect the positions of the funding organizations.

References

Blendermann, W., 1994. Parameter identification of wind loads on ships. J. Wind Eng. Ind. Aerod. 51 (3), 339–351.
Chen, Z.S., Lam, J.S.L., Xiao, Z., 2023. Prediction of harbour vessel fuel consumption based on machine learning approach. Ocean Eng. 278, 114483.
Choi, J.E., Min, K.S., Kim, J.H., Lee, S.B., Seo, H.W., 2010. Resistance and propulsion characteristics of various commercial ships based on CFD results. Ocean Eng. 37 (7), 549–566.
Coraddu, A., Lim, S., Oneto, L., Pazouki, K., Norman, R., Murphy, J., 2019a. A novelty detection approach to diagnosing hull and propeller fouling. Ocean Eng. 176, 65–73.
Coraddu, A., Oneto, L., Baldi, F., Cipollini, F., Atlar, M., Savio, S., 2019b. Data-driven ship digital twin for estimating the speed loss caused by marine fouling. Ocean Eng. 186.
Du, Y., Chen, Y., Li, X., Schönborn, A., Sun, Z., 2022a. Data fusion and machine learning for ship fuel efficiency modeling: part II–Voyage report data, AIS data and meteorological data. Commun. Transport. Res. 2, 100073.
Du, Y., Chen, Y., Li, X., Schönborn, A., Sun, Z., 2022b. Data fusion and machine learning for ship fuel efficiency modeling: part III– sensor data and meteorological data. Commun. Transport. Res. 2, 100072.
Erol, E., Cansoy, C.E., Aybar, O.Ö., 2020. Assessment of the impact of fouling on vessel energy efficiency by analyzing ship automation data. Appl. Ocean Res. 105.
Fan, A., Wang, Y., Yang, L., Yang, Z., Hu, Z., 2025. A novel grey box model for ship fuel consumption prediction adapted to complex navigating conditions. Energy 315, 134436.
Gao, Y., Tan, Y., Jiang, D., Sang, P., Zhang, Y., Zhang, J., 2025. An adaptive prediction framework of ship fuel consumption for dynamic maritime energy management. J. Mar. Sci. Eng. 13, 409.
Guo, Y., Lang, X., Wang, Y., Zhang, X., Zhao, X., Fu, S., Mao, W., 2026. State-of-the-art machine learning applications for ship performance modeling: a comprehensive review from design and operation to maintenance and retrofit. Appl. Energy 414, 127829.
Gupta, P., Rasheed, A., Steen, S., 2022. Ship performance monitoring using machine learning. Ocean Eng. 254.
Holtrop, J., Mennen, G.G.J., 1982. An approximate power prediction method. Int. Shipbuild. Prog. 29 (335), 166–170.
IMO, 2020a. Fourth Greenhouse Gas Study 2020.
IMO, 2020b. Just in Time Arrival Guide Barriers and Potential Solutions. https://greenvoyage2050.imo.org/wp-content/uploads/2021/01/GIA-just-in-time-hires.pdf. (Accessed 15 June 2023).
International Organization for Standardization, 2015. Ships and Marine Technology — Guidelines for the Assessment of Speed and Power Performance by Analysis of Speed Trial Data. ISO 15016:2015).
ITTC, 2002. Resistance uncertainty analysis, example for resistance test. Venice, Italy: Proceedings of the 23th International Towing Tank Conference (ITTC).
ITTC, 2014. Analysis of speed/power Trial Data. Recommended procedures and guidelines 7.5-04-01-01.2.
Kevin, N.U.S.A., Kodak, G., 2023. Comparison of maritime and road transportations in emissions perspective: a review article. Int. J. Electron. Govern. 10 (2), 48–60.
Kim, Y.R., Steen, S., Kramel, D., Muri, H., Strømman, A.H., 2023. Modelling of ship resistance and power consumption for the global fleet: the MariTEAM model. Ocean Eng. 281, 114758.
Lan, T., Huang, L., Ma, R., Wang, K., Ruan, Z., Wu, J., Li, X., Chen, L., 2025. A robust method of dual adaptive prediction for ship fuel consumption based on polymorphic particle swarm algorithm driven. Appl. Energy 379, 124911.
Lang, X., Mao, W., 2020. A semi-empirical model for ship speed loss prediction at head sea and its validation by full-scale measurements. Ocean Eng. 209, 107494.
Lang, X., Wu, D., Mao, W., 2024. Physics-informed machine learning models for ship speed prediction. Expert Syst. Appl. 238, 121877.
Lang, X., Zhang, M., Mao, W., Ringsberg, J.W., Tsoulakos, N., 2026. Physics-guided machine learning for ship biofouling assessment in support of maritime decarbonization. Transport. Res. Transport Environ. 156, 105364.
Luo, X., Zhang, M., Han, Y., Yan, R., Wang, S., 2025. Ship fuel consumption prediction based on transfer learning: models and applications. Eng. Appl. Artif. Intell. 141, 109769.
Manderbacka, T., Haranen, M., 2018. Feedback to design power requirements from statistical methods applied to onboard measurements. In: Marine Design XIII, vol. 2. CRC Press, pp. 917–922.
Matusiak, J., 2021. Dynamics of a Rigid ship-with Applications. Aalto University, Espoo, Finland.
Min, K.S., Kang, S.H., 2010. Study on the form factor and full-scale ship resistance prediction method. J. Mar. Sci. Technol. 15, 108–118.
Molland, A.F., Turnock, S.R., Hudson, D.A., 2017. Ship Resistance and Propulsion. Cambridge university press.
Piao, S., Park, M.-H., Yeo, S., Chun, K.W., Jee, J.-H., Lee, W.-J., 2025. Expanding the range of ship fuel consumption prediction: a multi-algorithm feature selection approach. Ocean Eng. 316, 119944.
Probha, N.A., Hoque, M.S., 2018. A study on transport safety perspectives in Bangladesh through comparative analysis of roadway, railway and waterway accidents. In: Proceedings of the Asia-Pacific Conference on Intelligent Medical 2018 & International Conference on Transportation and Traffic Engineering 2018, pp. 81–85.
Schultz, M.P., 2007. Effects of coating roughness and biofouling on ship resistance and powering. Biofouling 23 (5), 331–341.
Taimuri, G., Matusiak, J., Mikkola, T., Kujala, P., Hirdaris, S., 2020. A 6-DoF maneuvering model for the rapid estimation of hydrodynamic actions in deep and shallow waters. Ocean Eng. 218, 108103.
Tillig, F., Ringsberg, J.W., 2019. A 4 DOF simulation model developed for fuel consumption prediction of ships at sea. Ships Offshore Struct. 14 (Suppl. 1), 112–120.
UNCTAD, 2023. Review of Maritime Transport 2023.
UNFCCC, 2022. Long-term low-emission development strategies. Synthesis report by the secretariat. Sharm el-Sheikh Clim. Change Conf.
Uzun, D., Demirel, Y.K., Coraddu, A., Turan, O., 2019. Time-dependent biofouling growth model for predicting the effects of biofouling on ship resistance and powering. Ocean Eng. 191.
Valchev, I., Coraddu, A., Kalikatzarakis, M., Geertsma, R., Oneto, L., 2022. Numerical methods for monitoring and evaluating the biofouling state and effects on vessels' hull and propeller performance: a review. Ocean Eng. 251.

Yan, R., Wang, S., Du, Y., 2020. Development of a two-stage ship fuel consumption prediction and reduction model for a dry bulk ship. Transport. Res. E Logist. Transport. Rev. 138, 101930.

Zhang, M., Taimuri, G., Zhang, J., Hirdaris, S., 2023. A deep learning method for the prediction of 6-DoF ship motions in real conditions. Proc. IME M J. Eng. Marit. Environ., 14750902231157852

Zhang, M., Tsoulakos, N., Kujala, P., Hirdaris, S., 2024. A deep learning method for the prediction of ship fuel consumption in real operational conditions. Eng. Appl. Artif. Intell. 130, 107425.